

STABILITY, FLIGHT CONTROL, AND ENERGY MANAGEMENT  
OF THE DYNA-SOAR GLIDER

By A. H. Lee and L. J. Mason  
Boeing Airplane Company

SUMMARY

This paper presents some of the stability and control characteristics of the Dyna-Soar glider based upon analysis and testing done during the phase I contract period. Flying qualities, with and without stability augmentation, and a method of outer loop control for energy management are described.

An adaptive control system is planned. The primary control mode is manual with pilot input commands through the stability-augmentation system. A second control mode is provided which couples the pilot directly with the actuation system, bypassing the stability-augmentation system. Flying qualities with stability augmentation correlate with the "desired response" region of the flying qualities requirements of reference 1. Unaugmented flying qualities satisfactory for emergency operation appear to be attainable.

Control of the vehicle velocity as a function of range to go is shown to be a feasible method of energy management to achieve range control.

INTRODUCTION

The wide range of flight conditions encountered during reentry and glide create unusual stability and control problems. In order to perform its mission, the glider must be capable of trimmed flight to angles of attack of about  $50^\circ$  at hypersonic speeds and must be capable of a conventional landing. Flying qualities satisfactory for pilot control with and without stability augmentation are desired throughout the flight regime.

From experience and, more recently, from investigations by the NASA and Air Force funded projects involving variable-stability aircraft, the desired handling qualities for piloted control are reasonably well known.

Preceding page blank


Minimum required flying qualities for pilot control are not as well defined. Recent investigations by the NASA and by the Cornell Aeronautical Laboratory under WADD contract have provided data on minimum handling qualities at low speeds. Results from these investigations, and others, have been compiled in reference 1 as a preliminary statement of handling-qualities requirements for hypervelocity aircraft. These requirements have been considered in developing Dyna-Soar handling qualities, although it is recognized that further studies are required to confirm their applicability to hypersonic conditions.

For conventional low-speed aircraft, desired flying qualities can be provided by proper tailoring of the configuration. For vehicles similar to the Dyna-Soar glider, configuration tailoring is less satisfactory. However, through the use of stability augmentation, desired handling qualities can be provided. Without stability augmentation, handling qualities satisfactory for emergency operation appear obtainable. A self-adaptive control system is planned to achieve the desired system response over the flight range and to facilitate blending of aerodynamic and reaction control forces. A specific guidance and control system, and therefore the specific adaptive technique, has not been selected for Dyna-Soar, and the controlled vehicle characteristics should be regarded as typical of what can be attained by using adaptive methods.



L  
1  
1  
1  
3

#### SYMBOLS

b	wing span, ft
$C_{1/2}$	number of cycles of oscillation to damp to half-amplitude
$C_2$	number of cycles of oscillation to double amplitude
$C_D$	drag coefficient, Drag/qS
$C_L$	lift coefficient, Lift/qS
$C_{L,MAX}$	maximum lift coefficient
$C_l$	rolling-moment coefficient, Rolling moment/qSb
$C_{l\beta} = \partial C_l / \partial \beta$	per degree
$C_n$	yawing-moment coefficient, Yawing moment/qSb
$C_{n\beta} = \partial C_n / \partial \beta$	per degree



$c_r$	reference wing root chord, ft
$f_n$	natural frequency, cps
$h$	altitude, ft
$\dot{h}$	rate of change of altitude, ft/sec
$I_x, I_z$	moments of inertia about conventional airplane X and Z body axes, respectively, slug-ft <sup>2</sup>
$K$	control-system gain
$L/D$	lift-drag ratio
$(L/D)_{MAX}$	maximum lift-drag ratio
$M$	Mach number
$p$	rolling velocity, radians/sec
$q$	pitching velocity, radians/sec; dynamic pressure, lb/sq ft
$R$	range, nautical miles
$S$	wing area, sq ft
$s$	Laplace transform operator
$V_M$	measured velocity, ft/sec
$V_O$	initial total velocity, ft/sec
$V_P$	programed velocity, ft/sec
$v_e$	equivalent velocity along conventional airplane Y body axis
$\alpha$	angle of attack, deg
$\beta$	angle of sideslip, deg
$\gamma_0$	initial flight-path angle, deg
$\zeta$	damping ratio of oscillatory mode of motion



$\phi$  roll angle, deg

$\omega_n$  natural frequency of oscillatory motion, radians/sec

## DISCUSSION

## Vehicle Stability Characteristics Without Augmentation

Longitudinal.- Aerodynamic-center estimates based on wind-tunnel tests during phase I are shown in figure 1 as functions of Mach number and lift coefficient. The center-of-gravity location, which is practically invariant during the flight, is 63 percent of the reference root chord. Positive stability is indicated for all normal flight conditions which are, in general, at lift coefficients above that for  $(L/D)_{MAX}$ . However, an instability is noted for lift coefficients below 0.08 at hypersonic speeds. Future studies will be directed toward improving this low-lift-coefficient stability. Possible means of improvement include a change in the forward body contour.

Folding wing-tip extensions that are a part of the vertical fin are used at subsonic speeds to reduce the transonic aerodynamic-center shift. As shown, the tip extensions move the subsonic aerodynamic centers rearward about 4 percent of the root chord. It may be possible to satisfy design objectives by means of other configuration features - for example, with a large nose incidence and large elevons. Future study supported by wind-tunnel tests will provide the final answer. However, at this date, folding wing-tip extensions appear to provide a favorable compromise between stability, control, aerodynamic heating, and performance requirements. Reasonably good stability is indicated during the nominal approach,  $C_L = 0.11$ , and landing,  $C_L = 0.25$ .

The unaugmented flying qualities of the glider are presented for representative speeds of the flight regime at maximum lift and maximum range conditions. These conditions are presented in figure 2 as  $C_{L,MAX}$  and  $C_L$  for  $(L/D)_{MAX}$  as a function of Mach number. At speeds below a Mach number of approximately 5,  $C_{L,MAX}$  is limited by the angle of attack for neutral static stability. Above a Mach number of approximately 5, it is limited by the wing lift capability.

The glider's longitudinal flying qualities without stability augmentation are presented in figure 3. The reference boundaries were obtained from reference 1. Since normal operation of the Dyna-Soar glider is with stability augmentation, the boundaries of interest for flight without augmentation are those for emergency operation. The

major source of data for these boundaries was an investigation with a variable-stability B-26 airplane. Most of the investigation was conducted during landing approaches. However, some tests under instrument flight conditions established essentially the same requirements.

The unaugmented flying qualities of the glider are reasonably good during landing. In fact, the damping and frequency are adequate for normal operation at the angle of attack for maximum L/D. As speed increases, both frequency and damping are reduced. At hypervelocities - Mach 20 is an example - unaugmented damping is essentially nonexistent. This condition is fundamental for any practical configuration. However, frequencies are also very low, about 0.1 cps at Mach 20, as shown in figure 4. Therefore, a pilot can provide damping through the proper phasing of his control inputs. It is noted that the flying qualities for supersonic and hypersonic speeds fall in the "acceptable for short-time emergency operation" category. Since this category was derived principally during landings, future studies are required to define the degree of its applicability to the high-altitude flight of this class of vehicles.

Lateral-directional stability and control.- Directional-stability and dihedral-effect derivatives,  $C_{n\beta}$  and  $C_{l\beta}$ , are presented in figure 5. The data are presented for conventional airplane body axes. Although this  $C_{n\beta}$  is a good representation of a vehicle's directional stability at low angles of attack, it has been shown in the paper by John W. Paulson, Robert E. Shanks, and Joseph L. Johnson that it is not necessarily representative of stability for the high angles of attack associated with the Dyna-Soar glider. A better representation is  $(C_{n\beta})_{\text{dynamic}}$ . This parameter is defined as

$$(C_{n\beta})_{\text{dynamic}} = C_{n\beta} - \frac{I_z}{I_x} C_{l\beta} \sin \alpha$$

For the glider,  $(C_{n\beta})_{\text{dynamic}}$  is significantly larger than  $C_{n\beta}$  at high angles of attack. The glider's directional stability and dihedral effect are positive except for a small negative dihedral effect for flight at maximum L/D at supersonic speeds.

The unaugmented lateral-directional flying qualities are presented in figure 6, correlated with handling qualities required for emergency operation. The boundaries were obtained from reference 1. Boundaries for emergency conditions were determined principally from tests with a variable-stability F-86 airplane making simulated landings at 10,000 feet.

As shown, lateral flying qualities for the glider are in the "acceptable (emergency)" category from landing through hypervelocity speeds. Low damping exists for all flight conditions. This is characteristic of aircraft with highly swept wings because of their high ratios of yaw moment of inertia to roll moment of inertia and their low roll damping. Lateral-oscillation frequencies during landing are approximately 0.3 cps. At Mach 20, the frequencies range from 0.3 cps at  $C_{L,MAX}$  to 0.2 cps at  $(L/D)_{MAX}$ , as shown in figure 7. The higher frequency at  $C_{L,MAX}$  stems from the stabilizing effect of  $C_{l\beta}$  at high angles of attack.

### Vehicle Stability Characteristics With Stability Augmentation

Longitudinal and lateral response and control-system gains for three representative flight conditions that cover the range of uncontrolled vehicle dynamics are shown in figure 8. The flight conditions are:

Condition	Mach number	q, lb/sq ft	$\alpha_{trim}$ , deg
Reentry (near zero damping)	15	25	41
Landing (near neutral stability)	.25	167	7.5
Approach (high-dynamic pressure)	.85	200	5.5

With the indicated gains, both longitudinal and lateral responses are nearly constant (about 0.5 cps and a damping ratio of 0.5 to 0.7). Longitudinal response was selected on the basis of "desired" handling-qualities requirements from reference 1. Longitudinal response characteristics, with and without stability augmentation, are shown in figure 9 relative to the desired response. The selected response with augmentation, toward the low-frequency and low-damping-ratio boundaries, was purposeful. Much higher control-system gains were required to provide longitudinal response at the center of the desired response region. Problems with regard to control-surface deflection limits would result and pilot commands would be restricted to avoid rate saturation.

The approach taken to achieve the desired longitudinal response is shown by the diagram at the top of figure 8. The analysis included reasonable assumptions for instrument and actuation system characteristics. A control function was determined by using pitch angular

L  
1  
1  
1  
3

acceleration, pitch angular rate, and lagged angular-rate feedbacks. The control function was mechanized in such a manner that only the forward gain was varied; the gains associated with angular acceleration, angular rate, and lagged angular rate were each changed in the same proportion. These proportions remained fixed for the entire flight. The variable gain element in the forward control loop must be adaptive and must be adjusted as a function of a particular error criterion, depending upon the adaptive method used. Pitch-axis gain changes of the order of 10:1 were required for the range of flight conditions shown.

L  
1  
1  
1  
3

A similar approach was used in mechanizing the lateral-directional control. Yaw rate and yaw angular acceleration (not shown in fig. 8) were used for yaw control. Roll rate and lagged roll rate were used for roll control. Gain ratios were formed which remained constant during the flight and only the forward gain parameter was varied in each axis. Roll gain changes of about 20:1 were required. However, the selected gains were slightly high, since the desired damping for normal operation (from fig. 6) was about 0.3 to 0.5 rather than 0.5 to 0.7 as shown in figure 8.

#### Flight-Path Control

One area of outer loop control that has received considerable attention is energy management or range control. As defined here, the problem is concerned with:

1. Range control by proper management of energy to insure that the vehicle arrives at the landing site within permissible tolerances
2. Correction of errors in initial conditions and range errors resulting from deviations from expected atmospheric properties and aerodynamic parameters
3. Control of the flight path to maintain a safe margin above the reentry heating boundary

The Dyna-Soar will be landed manually with visual, voice, or radar contact with ground. Therefore, the problem of energy management is concerned with the period of flight from boost termination to a terminal position and velocity from which landing can be accomplished. In phase I studies, this was assumed to be a 100,000-foot altitude and a velocity of 4,000 ft/sec. Between these limits the stored energy is almost totally kinetic and some form of velocity control appears desirable. Velocity control as a function of range to go proved satisfactory. Control was achieved by varying the vehicle angle of attack to change lift and drag forces.

This range-control concept is illustrated in figure 10. The nominal flight path lies approximately midway between the trajectories for  $C_{L,MAX}$  and  $C_L$  for  $(L/D)_{MAX}$ . The angle of attack required for the nominal path is programmed before the flight as a function of velocity or range to go. In figure 10, the vehicle is shown off the nominal path at a velocity less than the programmed velocity. If the vehicle continued to fly the nominal angle-of-attack program, it would fall short of the desired terminal condition. Path corrections are made in the following manner. A change in angle of attack  $\Delta\alpha$  is computed from comparison of the measured or actual velocity  $V_M$  and the programmed velocity  $V_p$ , where  $V_p$  is a function of the range to go. For the condition shown in figure 10, the commanded angle of attack would be reduced from the nominal value. With this change, the vehicle would fly at a higher  $L/D$  to reduce the velocity error to zero.

Damping of the altitude oscillation is provided by a function of altitude rate  $\dot{h}$ . Altitude rate, temperature rate, and forward acceleration are each a possible data source of the proper phase to provide the damping function. Altitude rate was selected because it is readily available from the inertial guidance system. Steady-state altitude rate signals would be filtered to avoid bias errors during the gliding descent. Since the vehicle seeks the right density for equilibrium glide, safe margin above the heating boundary at hypersonic speeds is inherent with this energy-management concept, provided altitude oscillations are adequately damped. Also, appropriate altitude limits relative to heating restrictions must be applied.

Flight-path stability and vehicle performance during reentry and glide, with velocity control used for energy management, are shown in figure 11. These examples were taken from analog simulation studies. Perfect guidance was assumed and trajectory calculations were based on a spherical earth. The terminal condition was an altitude of 100,000 feet and a velocity of 4,000 ft/sec. Controlled reentry trajectories with excessively large initial velocity errors of -300 and 200 ft/sec from the nominal initial velocity of 23,800 ft/sec are shown to indicate the control capability. In this series of tests the vehicle angle of attack was changed as a function of range error, that is, the difference between predicted range (based on the nominal programmed path) and required range (based on knowledge of present position and destination).

The information in figure 11 is repeated in figure 12 in terms of velocity and altitude. It can be seen that the vehicle is controlled to a safe margin above the heating limit with altitude response well damped in spite of the very large initial velocity error. From these simulation tests, it was concluded that the controlled vehicle was



stable and could accommodate the range of reentry errors shown in table I with less than 2 percent error in velocity and altitude at zero range to go:

To this point the discussion has been of the reentry phase. Actually, range control must be continuous from launch. So far as the glider alone is concerned, range control must be initiated immediately after boost termination. As shown in the paper by James S. Lesko, the total range control available after boost termination (for the nominal once-around mission; launch at Cape Canaveral to landing at Edwards Air Force Base) was 21,000 nautical miles and -10,000 nautical miles. After reentry the range-control capability was reduced to about  $\pm 3,000$  nautical miles. Range errors resulting from tolerances in end-of-boost conditions and possible deviations from standard atmospheric properties and expected aerodynamic drag are summarized in table II. The predominant error sources, air density and predicted vehicle drag coefficient, define the requirement for initiating glider range control immediately after boost termination since the possible error exceeds the control available after reentry. The effectiveness of the range control system, velocity controlled as a function of range to go, in minimizing range errors during flight from the end of boost to reentry is shown in table III. As in the study of the reentry phase, perfect guidance was assumed. Trajectory calculations are based on a spherical rotating earth.

#### CONCLUDING REMARKS

Desired handling qualities can be provided throughout the flight regime with stability augmentation. Handling qualities of the basic vehicle without stability augmentation appear satisfactory for emergency operation. However, additional work is required to define minimum handling-qualities requirements more precisely for hypervelocity gliders. As additional knowledge on the requirements is gained, it will be applied to the configuration development.

Flight control and guidance systems have not been selected for the Dyna-Soar vehicle. Controlled-vehicle characteristics have been presented as typical of those that can be attained by adaptive flight-control system.

The energy-management system in which velocity control is used as a function of range to go is shown to be feasible and must function from the end of boost for adequate range control. Perfect guidance accuracy was assumed in the data presented. A guidance error analysis has also



been made for the Dyna-Soar. Summarizing from the paper by James S. Lesko, the principal guidance errors are reflected in range errors of  $\pm 2$  nautical miles downrange and  $\pm 6$  nautical miles crossrange for the nominal once-around mission.

REFERENCE

1. Breuhaus, W. O., Reynolds, P. A., and Kidd, E. A.: Handling Qualities Requirements for Hyper-Velocity Aircraft. Rep. No. TC-1332-F-1 (Preliminary), Cornell Aero. Lab., Inc., Sept. 30, 1959.

L  
1  
1  
1  
3



TABLE I  
RANGE CONTROL  
AFTER REENTRY

REENTRY CONDITION	—————→		TERMINAL CONDITION
ALTITUDE, FT	400,000 ± 100,000		100,000 ± 2,000
VELOCITY, FPS	23,800 + 200 - 300		4,000 ± 80
FLIGHT-PATH ANGLE, DEG	0 ± .5		

TABLE II  
RANGE ERRORS  
ONCE-AROUND MISSION

ERROR SOURCE	3σ ERROR	RESULTING RANGE ERROR, NAUT. MI.	
		Positive	Negative
DRAG COEFFICIENT	-10% 10%	2,100	-1,800
DENSITY	-50% 50%	6,000	-2,400
VELOCITY AT BOOST BURNOUT	-9 FPS 9 FPS	800	-800
FLIGHT PATH ANGLE AT BOOST BURNOUT	-.012° .012°	200	-200
ALTITUDE AT BOOST BURNOUT	-1,000 FT 1,000 FT	400	-400
OVERALL 3σ RANGE ERROR:		6,400	-3,100



TABLE III  
RANGE CONTROL  
END OF BOOST TO REENTRY (23,000 FPS)

CONDITION	Δ RANGE, NAUTICAL MILES	
	NO CONTROL	CONTROLLED
Δ DENSITY, PERCENT { 50 -50	-2,332 5,724	-16.3 0
Δ C <sub>D</sub> , PERCENT { 10 -10	-1,650 1,810	8.2 - .7



TRIMMED AERODYNAMIC CENTERS

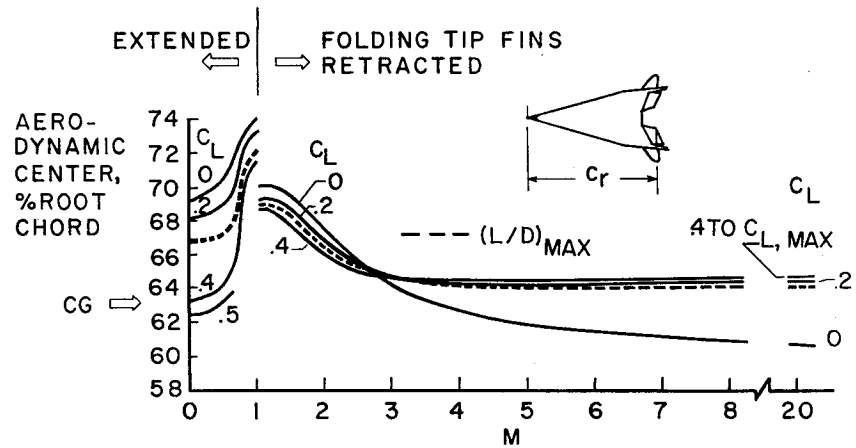


Figure 1

TRIMMED LIFT COEFFICIENT

$(\frac{L}{D})_{MAX}$  AND  $C_{L,MAX}$

--- FOLDING TIPS EXTENDED  
 — FOLDING TIPS RETRACTED

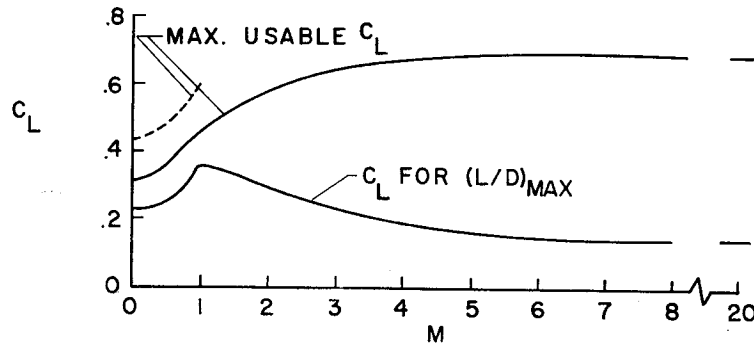


Figure 2

LONGITUDINAL SHORT-PERIOD FLYING QUALITIES  
NO STABILITY AUGMENTATION

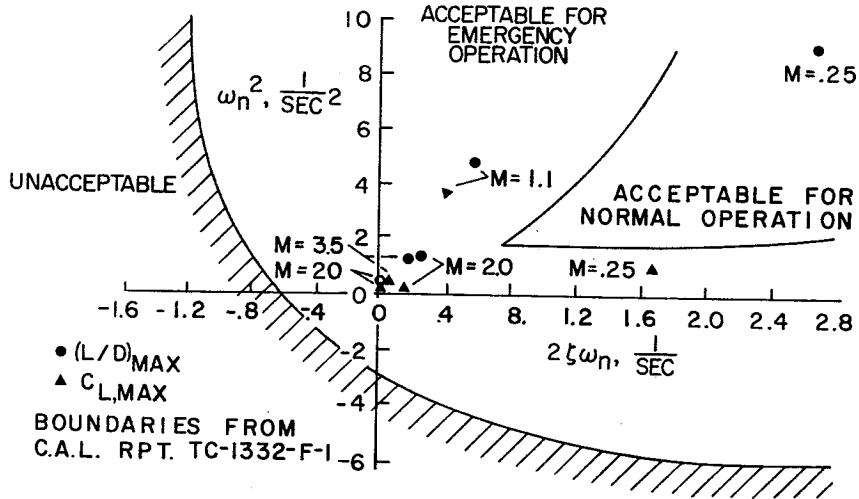


Figure 3

LONGITUDINAL SHORT-PERIOD DYNAMICS  
NO STABILITY AUGMENTATION

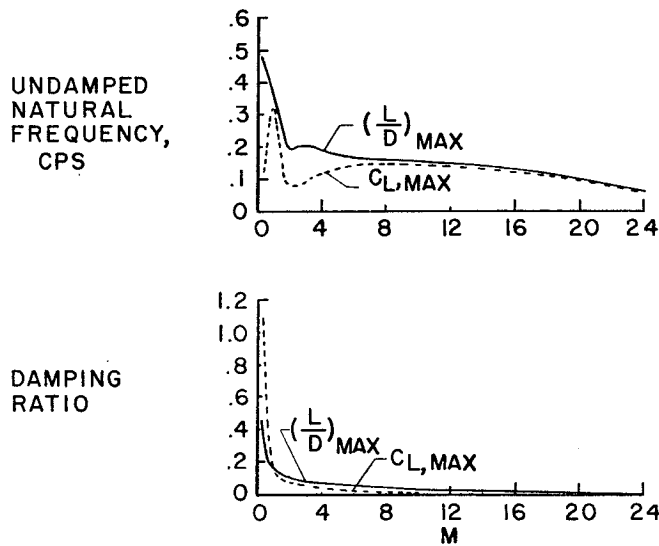


Figure 4

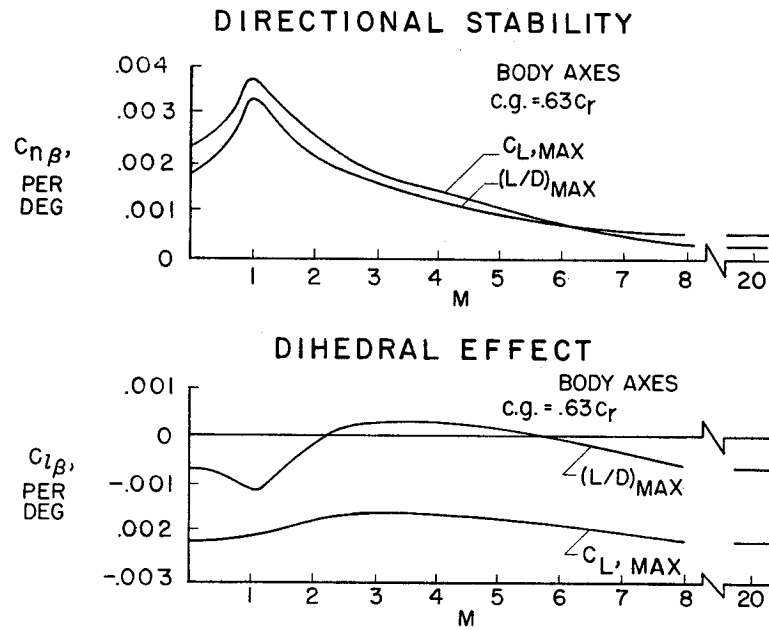


Figure 5

**LATERAL-DIRECTIONAL FLYING QUALITIES**  
NO STABILITY AUGMENTATION

BOUNDARIES FROM C.A.L. RPT. TC-1332-F-1

- $(\frac{L}{D})_{MAX}$  CONDITIONS
- ▲  $C_{L,MAX}$  CONDITIONS

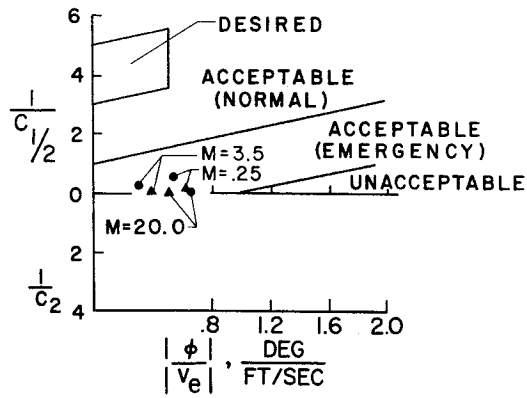


Figure 6

LATERAL OSCILLATION DYNAMICS  
NO STABILITY AUGMENTATION

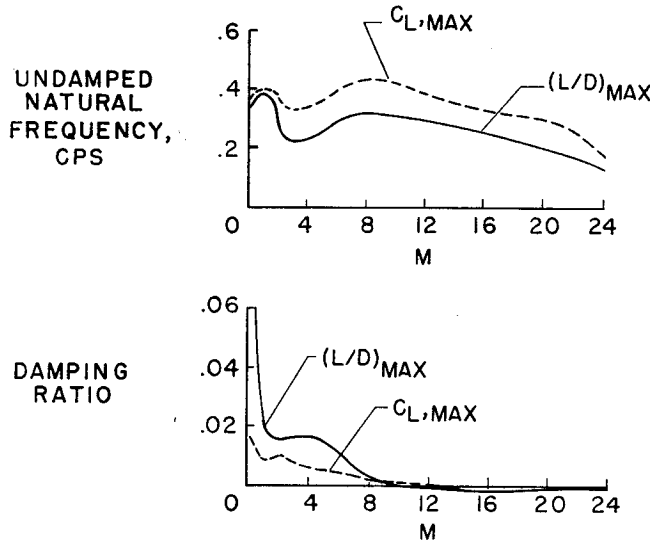
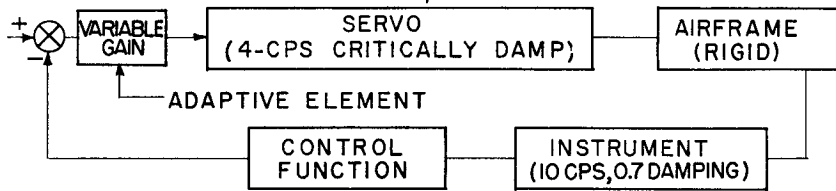


Figure 7

LONGITUDINAL AND LATERAL HANDLING  
QUALITIES WITH AUGMENTATION



MODE	FLIGHT CONDITION	RESPONSE		ADAPTIVE ELEMENT	CONTROL FUNCTION
		$f_n$ , CPS	$\zeta$		
LONGITUDINAL	REENTRY	0.46	0.49	5.0	$\frac{s^2}{10} + s + \frac{2s}{s+0.3}$
	APPROACH	.52	.61	.3	
	LANDING	.46	.58	.52	
LATERAL	REENTRY	0.5	0.5	2.1	$s + \frac{19s}{s+0.3}$ (RUDDER LOOP CLOSED)
	APPROACH	.46	.68	.11	
	LANDING	.53	.63	.14	

Figure 8



### LONGITUDINAL SHORT-PERIOD FLYING QUALITIES WITH STABILITY AUGMENTATION

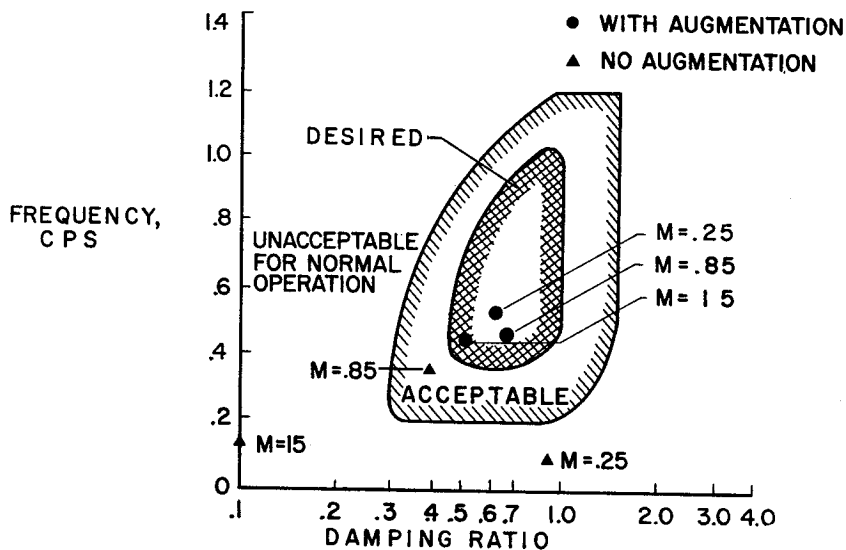


Figure 9

### ENERGY-MANAGEMENT CONCEPT

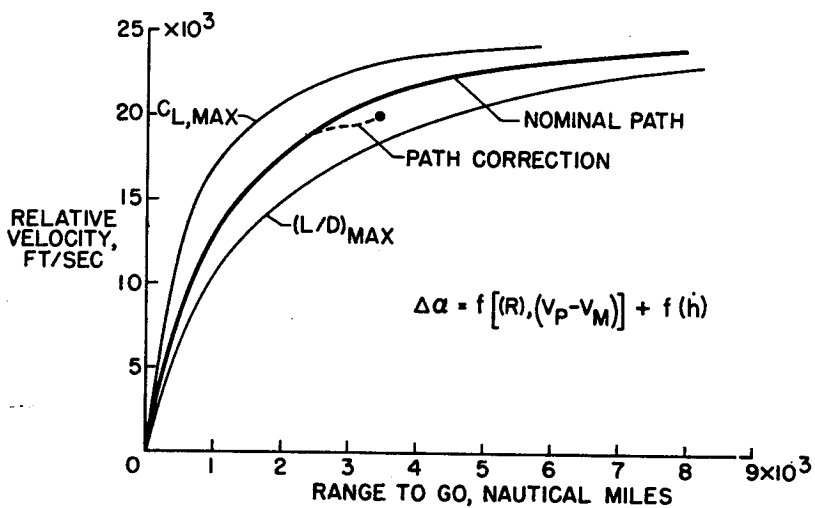


Figure 10

CONTROLLED GLIDER REENTRY

INITIAL CONDITIONS:  $h = 400,000$  FT;  $\gamma_0 = 0^\circ$ ;  $\alpha = 44.3^\circ$

RANGE TO GO, NAUT. MI.

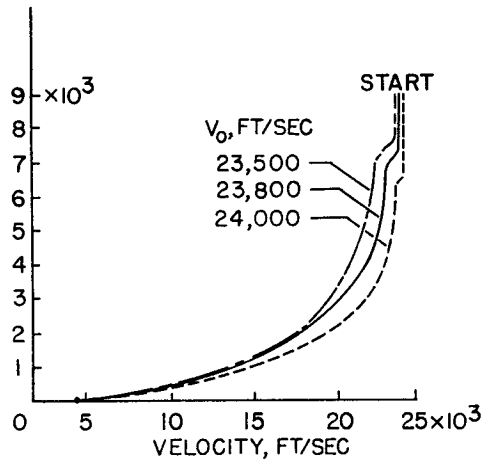


Figure 11

CONTROLLED GLIDER REENTRY

INITIAL CONDITIONS:  $h = 400,000$  FT;  $\gamma_0 = 0^\circ$ ;  $\alpha = 44.3^\circ$

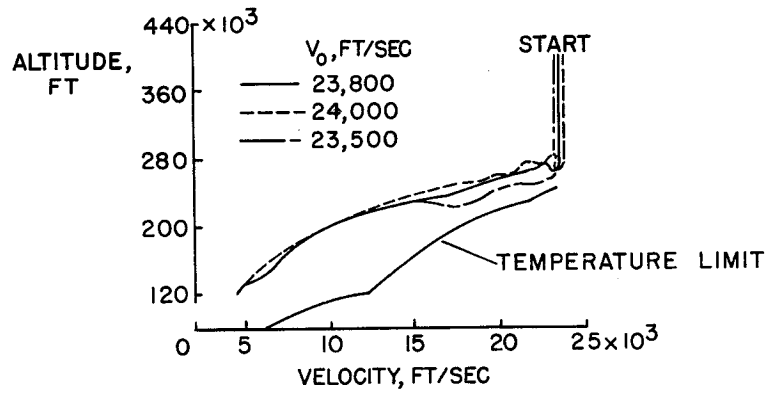


Figure 12